



Proceeding Paper

Nanostructured Copper Oxide Materials for Photocatalysis and Sensors [†]

Natalia Chirkunova 1,2, Amani Azaizia 2, Semen Domarev 3 and Maksim Dorogov 2,*

- ¹ Institute of Advanced Technologies, Togliatti State University, Togliatti 445020, Russia; natchv@yandex.ru
- ² Institute of Advanced Data Transfer Systems, ITMO University, St. Petersburg 197101, Russia; amaniazaizia.1997@mail.ru
- ³ International Research and Education Centre for Physics of Nanostructures, ITMO University, St. Petersburg 197101, Russia; sndomarev@itmo.ru
- * Correspondence: mvdorogov@itmo.ru
- [†] Presented at the 12th International Electronic Conference on Sensors and Applications (ECSA-12), 12–14 November 2025; Available online: https://sciforum.net/event/ECSA-12.

Abstract

This study investigates the influence of morphology on the photocatalytic and gas-sensing properties of copper oxide (CuO) nanomaterials, comparing spherical nanoparticles (NPs) and nanowhiskers (NWs). CuO NWs were synthesized via thermal oxidation of electro-deposited copper, exhibiting a polycrystalline structure with an average diameter of 68 nm, while NPs were obtained by ball-milling NWs, resulting in spherical particles (220 nm). Photocatalytic tests using methylene blue degradation under UV and visible light revealed that NWs exhibited superior. Kinetic analysis indicated pseudo-first-order behavior under visible light, while UV-driven reactions deviated due to surface-limited processes. In gas-sensing experiments, CuO NPs demonstrated higher sensitivity to acetone than NWs.

Keywords: copper oxide; nanowhiskers; nanoparticles; photocatalysis; gas sensors

1. Introduction

Rapid scientific and technological progress has led to the development of industrial production, such as chemical, mechanical engineering, automotive, electronics, etc. In the 21st century, we have witnessed not only the rapid development of industry and technology, but also a responsible attitude to nature and the transition to green technologies [1]. Industrial and automobile exhaust gases, domestic and industrial wastewater, pesticides used in agriculture, etc. are sources of pollutants and can cause serious environmental pollution, which poses a serious threat to human health. Therefore, there is an urgent need for both precise control of the types and concentrations of hazardous pollutants and technologies for their processing into safe compounds [2].

Photocatalysis is considered to be one of the most effective approaches to environmental remediation because organic pollutants are decomposed into harmless components such as carbon dioxide, water and inorganic non-toxic gases [3]. There are a number of suitable semiconductors for use as photocatalysts, such as iron oxide, copper oxide, zinc oxide, titanium dioxide [4]. These materials are also used in gas detection technology, which has attracted much attention in the industrial field due to its reliable performance and high sensitivity. In addition, gas detection also has great potential in other fields such

Academic Editor(s): Name

Published: date

Citation: Chirkunova, N.; Azaizia, A.; Domarev, S.; Dorogov, M. Nanostructured Copper Oxide Materials for Photocatalysis and Sensors. *Eng. Proc.* 2025, volume number, x. https://doi.org/10.3390/xxxxx

Copyright: © 2025 by the authors. Submitted for possible open access publication under the terms and conditions of the Creative Commons Attribution (CC BY) license (https://creativecommons.org/license s/by/4.0/).

as medicine, for example, with the development of modern medicine, it has been demonstrated that endogenous ammonia in exhaled air is an important biomarker for non-invasive diagnosis of chronic kidney disease [5].

Depending on the detection principle, gas sensors can be divided into electrochemical, resistive and optical. Resistive gas sensors have been widely studied due to their simple design, small size and high sensitivity. As a rule, the gas detection mechanism is based on the migration of charge carriers in the adsorption-desorption process, which leads to a number of changes in electrical parameters. It should be noted that for semiconductor resistive gas sensors, conductivity is the main parameter [6].

There are several parameters that influence the performance of a gas sensor, including sensitivity, selectivity, response and recovery time, and stability. The four main parameters are defined as follows [7].

Sensitivity (*Sen*) is the smallest amount of target gas that a gas sensor can detect (high sensitivity indicates high response).

The change in resistance ($\Delta R/R_0$) in a chemoresistive sensor is calculated by the formula:

$$Sen = \frac{R - R_0}{R_0} \cdot 100\%, \tag{1}$$

where R_0 and R are the resistance before and after exposure to gas molecules, respectively. Selectivity is the ability of a sensor to distinguish specific analytes from other components that exhibit similar behavior in a mixture.

Response/Recovery Time: The performance of a sensor is characterized by the response time and recovery time, which are the time it takes for the sensor to achieve 90% of the total change in resistance during adsorption and desorption, respectively.

Stability indicates whether the sensor response remains unchanged after repeated exposure to a given gas concentration.

Improving a gas sensor means improving some or all of these important parameters, which are largely determined by the materials used [8]. At present, several types of sensing materials are used to fabricate resistance-based gas sensors, including conductive polymers, metal oxides, two-dimensional (2D) materials, carbon-based materials, and transition metal carbides and nitrides [6]. We would like to highlight metal oxides, which are widely studied and developed due to their high chemical and thermal stability, low cost, and compatibility with modern electronic devices [9]. In particular copper oxide nanoparticles (CuO NPs) have emerged as a cornerstone material in modern sensing technologies due to their exceptional physicochemical properties. As a p-type semiconductor with a narrow bandgap (1.2–2.1 eV), CuO NPs exhibit remarkable electronic, optical, and catalytic characteristics that make them ideal for diverse sensing applications [10,11]. The growing demand for high-performance, cost-effective sensors in environmental monitoring, healthcare diagnostics, and industrial safety has driven extensive research into CuO-based nanomaterials.

It is important to note that, like photocatalysis processes, the operating principle of resistive gas sensors is associated with the phenomenon of adsorption and desorption of gas molecules on the surface of the active material. It is known that the number of active reaction centers with different morphologies can to a certain extent affect the efficiency of both the photocatalytic active and sensitive material. The well-known Barsan model of gas-sensitive behavior of p-type metal oxides describes the sensor response (*S*-signal) as follows [12]:

$$S = \frac{{}^{R}gas}{{}^{R}air} = \frac{\frac{L_{D}}{D_{C}}e^{\frac{-qV_{air}}{2kT}}e^{\frac{\Delta\Phi}{2kT}} + \frac{1}{1 + \frac{L_{D}}{D_{G}}e^{\frac{qV_{air}}{2kT}}e^{-\frac{\Delta\Phi}{2kT}}}}{\frac{L_{D}}{D_{C}}e^{\frac{-qV_{air}}{2kT}} + \frac{1}{1 + \frac{L_{D}}{D_{C}}e^{\frac{qV_{air}}{2kT}}}},$$
 (2)

where R_{gas} and R_{air} are the resistances of the sensor in the background gas and target gas, respectively, L_D is the Debye length (which determines the depletion region of the material), D_G is the grain size, D_G is the effective contact area, qV_{air} is the potential barrier in the air background gas, and $\Delta\Phi$ is the potential barrier difference between the target gas and the background gas.

The purpose of this work is to study the influence of morphology on photocatalytic activity and sensitivity of materials to volatile organic compounds using copper oxide in the form of spherical nanoparticles and nanowhiskers as an example.

2. Materials and Methods

2.1. Preparation of Active Material

Copper oxide nanoparticles and nanowhiskers were obtained in two steps. At the first step copper coating was prepared by electrodeposition using sulfurous copper electrolyte (250 g/L of copper sulfate and 90 g/L of sulfuric acid), the copper anode, and a substrate in the form of stainless-steel mesh with cell size 40 μ m and 30 μ m diameter wire. The mesh was purified by alcohol and distilled water in ultrasonic bath. Electrolysis was conducted at room temperature in a two-electrode cell using a potentiostat-galvanostat (P45-X, Electrochemical Instruments) in galvanostatic regime with current density 20 mA/cm² and electrodeposition time 5 h. At second step to obtain nanowhisker structures the sample was heat treated in air in a muffle furnace at 400 °C for 4 h after plating. Prepared nanowhiskers were separated from the mesh surface by treatment in an ultrasonic bath at 35 kHz frequency and power of 50 W for 1 h.

Copper oxide nanoparticles were obtained by grinding copper oxide nanowhiskers in a planetary ball mill (PM 100, Retsch) for 2 h at a rotation speed of 550 rpm.

2.2. Material Characterisation

The chemical composition of CuO nanoparticles and nanowhisker was determined by the energy-dispersive X-ray analysis (EDX-8000, Shimadzu). The morphology of such active nanomaterials was studied using the field emission scanning electron microscopy (MIRA-3, Tescan). The crystal structure and phase composition were studied using an X-ray diffractometer (DRON-8, Burevestnik). The diffuse-reflection spectra of the photocatalytically active materials were measured using a spectrophotometer (LAMBDA 1050, PerkinElmer) equipped with a 150 mm integrating sphere accessory.

2.3. Photocatalytic Test

Photocatalytic activity of the CuO nanomaterials was investigated using a model organic pollutant—methylene blue (MB). A conventional batch reactor equipped with a magnetic stirrer, air compressor with aerator and fluorescent light lamp (with a light filter for 400–746 nm) or UV DRUF-125 lamp was used for photocatalytic tests. The MB concentration in the solution was determined by the photometric method using a UV-Vis spectrophotometer (UV-2600, Shimadzu). The photocatalyst was pre-dispersed for 10 min in the MB solution using an ultrasonic bath. At the first stage, the sorption equilibrium was established (by keeping in a dark box for 30 min); then the radiation source was switched on in order to perform the photocatalysis, and the MB concentration was detected every 30 min.

2.4. Sensoring Test

Sensoring test using an electrical measurement was performed using a homemade experimental setup with a chamber (~2 cm³ volume) designed to accommodate the sample, a syringe pump providing accurate and controlled gas mixture supply to the chamber, and a meter (Keithley 2336B, Tektronix) connected to the sample electrodes for electrical characterization. Active material samples (copper oxide nanoparticles and nanowhiskers) were drop-coated onto Ossila glass-ITO substrates pre-coated with a graphene oxide layer.

3. Results and Discussion

Thermal oxidation of copper results in the growth of CuO nanowhiskers. Presumably, the formation of CuO nanowhiskers occurs as a result of a reaction at the CuO/Cu₂O interface, which creates compressive stresses in the CuO layer and leads to forced diffusion of copper ions outward along the boundaries of CuO grains [13]. Scanning electron microscopy (SEM) analysis of the nanowhiskers removed using ultrasound from the oxidized surface shows that the average diameter is 68 nm (see Figure 1). Our studies of cross-sections of the nanowhiskers with help high-resolution electron microscopy showed [14] that in most cases the nanowhiskers have a monoclinic lattice and a bicrystal or polycrystalline structure with a growth direction [110].

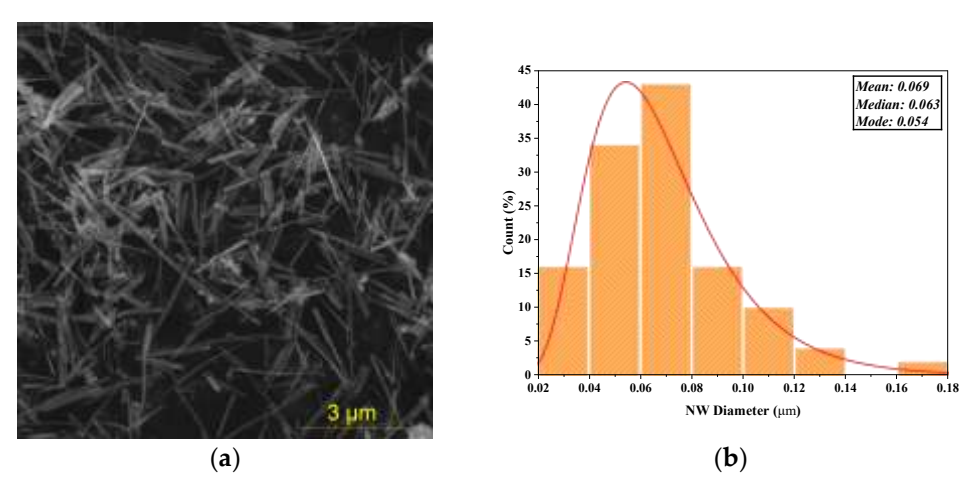


Figure 1. SEM photo of CuO nanowhiskers (a) and size distribution histogram (b).

Grinding of CuO nanowhiskers in a ball mill leads to their fragmentation and subsequent aggregation, resulting in the formation of slightly larger particles with a shape close to spherical. Statistical analysis of SEM data shows an average particle size of 220 nm.

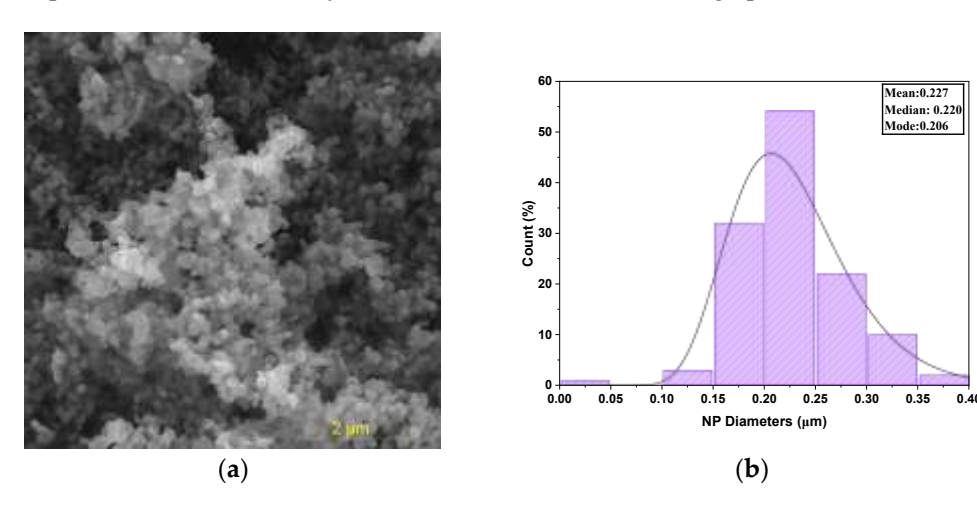


Figure 2. SEM photo of CuO nanoparticles (a) and size distribution histogram (b).

The X-ray diffraction analysis data shows that the obtained copper oxide powders in the form of nanoparticles and nanowhiskers contain only the CuO phase. Optical spectrometry using the diffuse reflectance method shows that after grinding the nanowhiskers to nanoparticles, no noticeable shift of the absorption band edge is observed, which is 863 and 866 nm for nanowhiskers and nanoparticles, respectively. The optical band gap calculated by the Tauc method [15] is ~1.3 eV for the studied material samples. The narrow band gap allows us to use such materials as a photocatalyst operating in the visible radiation range.

We conducted studies of the decomposition of an aqueous solution of MB in the presence of the obtained nanoparticles or nanowhiskers of CuO, both under UV and Vis part of the spectrum radiation. The kinetics of photocatalytic decomposition of MB is presented in Figure 3.

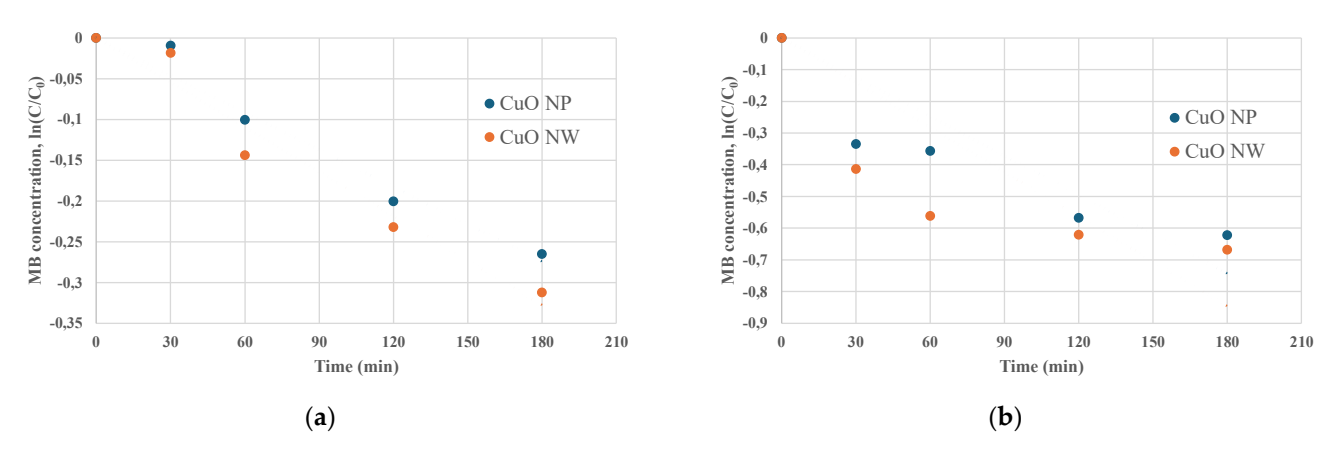


Figure 3. Plots of $\ln C_0/C$ as a function of reaction time (min) under Vis (a) and UV (b) radiation.

The degradation kinetics of methylene blue (MB) was studied according to the pseudo-first-order kinetic model, which can be represented by Equation (3):

$$\ln\frac{c_0}{c} = k_1 t, \tag{3}$$

where C_0 and C represent the MB concentrations at the initial stage (time zero) and at time t, respectively. The plots of $\ln(C_0/C)$ versus time (t) for the degradation of MB in its aqueous solution are shown in Figure 3. The rate constant (t1) of MB degradation was obtained from the slope of the corresponding plot. The half-life (t1/2) of MB in solution was obtained using following equation:

$$t_{1/2} = \frac{\ln 2}{k_1}. (4)$$

A good applicability of the pseudo-first order kinetic model for the photocatalytic degradation of MB under visible light is observed. The observed deviation from the pseudo-first order kinetic model in the case of UV irradiation may be due to the fact that in this case the limiting stage may be the surface reaction. The decomposition rate constants k_1 and $t_{1/2}$ and the characteristics of the photocatalyst such as the average particle diameter ($\langle D \rangle$), absorption edge (λ_{ae}), and band gap width (E_g) are given in Table 1.

Photocatalyst	< <i>D</i> >, nm	λ _{ae} , nm	E _s , eV	UV-Radiation		Vis-Radiation	
				<i>k</i> ₁, min⁻¹	<i>t</i> _{1/2} , min	k₁, min⁻¹	<i>t</i> _{1/2} , min
CuO NP		866	1.3	0.0041	169	0.0015	462
CuO NW	69	863	1.3	0.0047	147	0.0018	385

Table 1. This is a table. Tables should be placed in the main text near to the first time they are cited.

In the experiment to measure the electrical responses to various analytes, the baseline signal was recorded for the first 0–50 s, then the analyte was introduced from about 50 to 83 s, and then removed from 83 to 116 s. This input-output cycle was repeated several times with an interval of 150 s to obtain statistically significant results. The recording of the response of active materials based on copper oxide using the model analyte acetone as an example is shown in Figure 4.

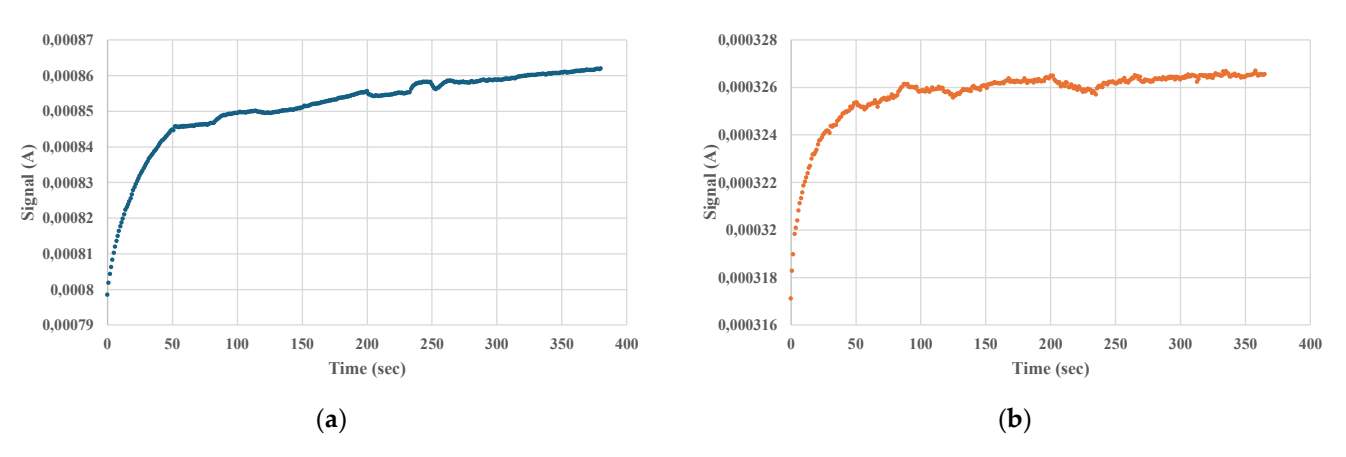


Figure 4. Electrical response to acetone of active material in the form of nanoparticles (a) and nanowhiskers (b).

Note that the response of the active material in the form of nanoparticles has a larger amplitude than that of the material in the form of nanowhiskers. In the case of photocatalysis, the opposite situation is observed—NWs are more active. This may be due to the different process environments—water and air; different reaction products, as well as the structural features and stress state of the active material [16].

4. Conclusions

This study investigated the influence of morphology on the photocatalytic and gassensing properties of copper oxide (CuO) nanomaterials, comparing spherical nanoparticles (CuO NPs) and nanowhiskers (CuO NWs). Both CuO NPs and NWs demonstrated visible-light-driven photocatalytic activity in the degradation of methylene blue (MB), following pseudo-first-order kinetics. Under UV irradiation, the reaction kinetics deviated from the pseudo-first-order model, suggesting a shift to a surface reaction-limited mechanism. CuO NWs exhibited superior photocatalytic efficiency compared to NPs, attributed to their higher surface area and enhanced charge-carrier mobility along the 1D structure. Resistive gas-sensing tests revealed that CuO NPs showed a higher response amplitude to acetone than NWs, likely due to their higher density of surface active sites. However, nanowhiskers may have advantages in terms of long-term stability and selectivity given their lower tendency to agglomerate.

Author Contributions: Conceptualization, N.C. and M.D.; methodology, N.C., A.A. and S.D.; software, A.A. and S.D.; validation, N.C. and M.D.; formal analysis, M.D.; investigation, N.C., A.A. and

S.D.; writing—original draft preparation, N.C. and M.D.; writing—review and editing, N.C. and M.D.; supervision, M.D. All authors have read and agreed to the published version of the manuscript.

Funding: This research was funded by the Ministry of Science and Higher Education of the Russian Federation, project number FSER-2025-0005.

Institutional Review Board Statement: Not applicable.

Informed Consent Statement: Not applicable.

Data Availability Statement: The original contributions presented in the study are included in the article material. Further inquiries can be directed to the corresponding author.

Conflicts of Interest: The authors declare no conflicts of interest.

References

- 1. Hickel, J.; Kallis, G. Is Green Growth Possible? New Polit. Econ. 2020, 25, 469–486.
- 2. Karimi-Maleh, H.; Darabi, R.; Karimi, F.; Karaman, C.; Shahidi, S.A.; Zare, N.; Baghayeri, M.; Fu, L.; Rostamnia, S.; Rouhi, J.; et al. State-of-art advances on removal, degradation and electrochemical monitoring of 4-aminophenol pollutants in real samples: A review. *Environ. Res.* **2023**, 222, 115338.
- 3. Aroob, S.; Carabineiro, S.A.C.; Taj, M.B.; Bibi, I.; Raheel, A.; Javed, T.; Yahya, R.; Alelwani, W.; Verpoort, F.; Kamwilaisak, K.; et al. Green Synthesis and Photocatalytic Dye Degradation Activity of CuO Nanoparticles. *Catalysts* **2023**, *13*, 502.
- 4. Kozlov, A.Y.; Dorogov, M.V.; Chirkunova, N.V.; Sosnin, I.M.; Vikarchuk, A.A.; Romanov, A.E. CuO Nanowhiskers-Based Photocatalysts for Wastewater Treatment. *Nano Hybrids Compos.* **2017**, *13*, 183–189.
- 5. Chen, C.-C.; Hsieh, J.-C.; Chao, C.-H.; Yang, W.-S.; Cheng, H.-T.; Chan, C.-K.; Lu, C.-J.; Meng, H.-F.; Zan, H.-W. Correlation between breath ammonia and blood urea nitrogen levels in chronic kidney disease and dialysis patients. *J. Breath Res.* **2020**, *14*, 036002.
- 6. Ding, Y.; Guo, X.; Zhou, Y.; He, Y.; Zang, Z. Copper-based metal oxides for chemiresistive gas sensors. *J. Mater. Chem. C* **2022**, 10, 16218–16246.
- Guo, S.-Y.; Hou, P.-X.; Zhang, F.; Liu, C.; Cheng, H.-M. Gas Sensors Based on Single-Wall Carbon Nanotubes. Molecules 2022, 27, 5381.
- 8. Khorramifar, A.; Karami, H.; Lvova, L.; Kolouri, A.; Łazuka, E.; Piłat-Rożek, M.; Łagód, G.; Ramos, J.; Lozano, J.; Kaveh, M.; et al. Environmental Engineering Applications of Electronic Nose Systems Based on MOX Gas Sensors. *Sensors* **2023**, 23, 5716.
- 9. Chen, H.; Chen, H.; Chen, J.; Song, M. Gas Sensors Based on Semiconductor Metal Oxides Fabricated by Electrospinning: A Review. *Sensors* **2024**, *24*, 2962.
- 10. Steinhauer, S. Gas Sensors Based on Copper Oxide Nanomaterials: A Review. Chemosensors 2021, 9, 51.
- 11. Maier, C.; Egger, L.; Köck, A.; Reichmann, K. A Review of Gas Sensors for CO2 Based on Copper Oxides and Their Derivatives. *Sensors* **2024**, 24, 5469.
- 12. Barsan, N.; Simion, C.; Heine, T.; Pokhrel, S.; Weimar, U. Modeling of sensing and transduction for p-type semiconducting metal oxide based gas sensors. *J. Electroceramics* **2010**, *25*, 11–19.
- 13. Dorogov, M.V.; Priezzheva, A.; Vlassov, S.; Kink, I.; Shulga, E.; Dorogin, L.; Lõhmus, R.; Tyurkov, M.; Vikarchuk, A.; Romanov, A. Phase and structural transformations in annealed copper coatings in relation to oxide whisker growth. *Appl. Surf. Sci.* **2015**, 346, 423–427.
- 14. Dorogov, M.; Kalmykov, A.; Sorokin, L.; Kozlov, A.; Myasoedov, A.; Kirilenko, D.; Chirkunova, N.; Priezzheva, A.; Romanov, A.; Aifantis, E.C. CuO nanowhiskers: Preparation, structure features, properties, and applications. *Mater. Sci. Technol.* **2018**, *34*, 2126–2135.
- 15. Tauc, J.; Grigorovici, R.; Vancu, A. Optical Properties and Electronic Structure of Amorphous Germanium. *Phys. Status Solidi* **1966**, 15, 627–637.
- 16. Dorogin, L.M.; Dorogov, M.V.; Vlassov, S.; Vikarchuk, A.A.; Romanov, A.E. Whisker Growth and Cavity Formation at the Microscale. *Rev. Adv. Mater. Technol.* **2020**, *2*, 1–31.

Disclaimer/Publisher's Note: The statements, opinions and data contained in all publications are solely those of the individual author(s) and contributor(s) and not of MDPI and/or the editor(s). MDPI and/or the editor(s) disclaim responsibility for any injury to people or property resulting from any ideas, methods, instructions or products referred to in the content.